Energy levels of mesonic helium in quantum electrodynamics

V. I. Korobov ⬤

BLTP JINR, Dubna 141980, Russia
and Physics Department, Samara National Research University, Samara 443086, Russia

A. V. Eskin ⬤, A. P. Martynenko ⬤, and F. A. Martynenko ⬤

Physics Department, Samara National Research University, Samara 443086, Russia

On the basis of the variational method we study the energy levels of pionic helium (π-e-He) and kaonic helium (K-e-He) with an electron in the ground state and a meson in the excited state with principal and orbital quantum numbers $n \sim l + 1 \sim 20$. Variational wave functions are taken in the Gaussian form. Matrix elements of the basic Hamiltonian and corrections to vacuum polarization and relativism are calculated analytically in a closed form. We calculate some bound-state energies and transition frequencies which can be studied in the experiment.

I. INTRODUCTION

One of the directions in the development of the theory of fundamental interactions is connected to the study of bound states of particles. In addition to the usual stable atoms and molecules that exist in our world, there are exotic bound states (muonium, positronium, positronium ions, muonic hydrogen, and others), which have attracted the attention of both experimenters and theoreticians for decades [1–3]. Although bound states have a short lifetime, by studying various energy intervals in the energy spectrum of such systems, as well as their decay widths, year after year, it was possible to obtain from these studies more accurate information about the values of the fundamental parameters of the standard model. The number of such exotic systems has been growing in recent years. For example, Refs. [4,5] proposed to study, using the laser spectroscopy method, pionic helium atoms, which consist of a negative pion, an electron, and a helium nucleus. From a measurement of pion transitions between states with large values for the principal and orbital quantum numbers $[(n, l) = (17.16) \rightarrow (17.15)]$ one can try to obtain a more accurate value of the pion mass than can be obtained with other methods. In [6,7], a successful experiment was already carried out for nearly circular orbits, $n \sim l + 1$, which gave a transition-frequency value of 183 760 MHz. To find a more accurate value of the pion mass from these measurements, it is also necessary to take into account systematic effects such as collision-induced shift and broadening of the transition lines, among others [8–10]. The work in this direction is in an active phase. Along with the atoms of pionic helium, other atoms can be proposed and studied, for example, kaonic helium, with the goal of research being a more accurate determination of the mass of the K^- meson. It is useful to note that there are other approaches to clarifying the value of the π meson mass. Thus, the study carried out in [11] demonstrated the potential of crystal spectroscopy of curved crystals in the field of exotic atoms. In that work, $5g$-$4f$ transitions in pionic nitrogen and muonic oxygen were measured simultaneously in a gaseous nitrogen-oxygen mixture. Knowing the muon

mass, the muon line can be used to energy calibrate the pion transition. The mass value of a negatively charged pion was obtained and is 4.2 ppm higher than the current world average of 139.570 77 ± 0.000 17 MeV [12].

Mesonic atoms are formed as a result of the replacement of an orbital electron by a negatively charged meson. After that, laser spectroscopy of such atoms will make it possible to measure transition frequencies and determine the reduced mass of the system and hence the mass of the meson. To reduce the influence of strong interaction between a meson and a nucleus, the meson's orbit is raised by increasing its orbital momentum. The long lifetime of a meson atom is determined by the state with a large value for the orbital momentum $l = (16/20)$ in which a meson is formed in the atom. Its transition to the ground state with $l = 0$ is strongly suppressed. The lifetime of such an atom is several nanoseconds.

The study of energy levels of three-particle systems can be carried out with high accuracy within the framework of the variational method. There are some differences in the use of the variational method to find the energy levels of three-particle systems. They are connected to the choice of coordinates and representation of the Hamiltonian to describe the system, with the choice of basis wave functions. Thus, in [4] an exponential basis was used, and the coordinates of the electron and meson were determined with respect to the nucleus. In Refs. [13–15], when calculating the energy levels of mesomolecules of hydrogen, muonic helium, etc., we used Jacobi coordinates. For systems with three or more particles, constructing a good set of basis functions is not an easy task, and calculating the matrix elements becomes a very labor-intensive process. From this point of view, Gaussian functions written in Jacobi coordinates are especially suitable for the analytical calculation of matrix elements and for obtaining the energies of the ground and excited states. The purpose of this work is to calculate the energy levels in pionic and kaonic helium atoms, as well as transition frequencies between levels in which the meson is in an excited state with a large orbital quantum number.

II. GENERAL FORMALISM

Different approaches have been developed for the study of three-particle systems. There is an analytical method of perturbation theory, which makes it possible to analytically investigate both the Lamb shift and the hyperfine structure of the spectrum [15–21]. Other methods that are used for many-particle systems are the variational method and the method of hyperspherical coordinates, which allow one to find energy levels and wave functions with very high accuracy [22–31]. Since, for mesonic helium, the states of an atom with large orbital moments for the meson are considered so that the electron and meson are the same distance from the nucleus, it is virtually impossible to use a method employing the analytical perturbation theory. Therefore, we study this system on the basis of the variational method. The Gaussian basis is used as the basis set for the wave functions.

To find the energy levels of a three-particle system, we introduce the Jacobi coordinates $\boldsymbol{\rho}$ and $\boldsymbol{\lambda}$, which are related to the particle radius vectors $\mathbf{r}_1$ (nucleus), $\mathbf{r}_2$ (meson), and $\mathbf{r}_3$ (electron) as follows:

$$\boldsymbol{\rho} = \mathbf{r}_2 - \mathbf{r}_1, \quad \boldsymbol{\lambda} = \mathbf{r}_3 - \frac{m_1 \mathbf{r}_1 + m_2 \mathbf{r}_2}{m_1 + m_2}, \tag{1}$$

where m_1, m_2, and m_3 are the masses of the He nucleus, π^- (K^-) meson, and electron.

To solve the variational problem, we choose the ground-state trial-basis wave functions in the form of the superposition of the Gaussian exponents:

$$\Psi(\boldsymbol{\rho}, \boldsymbol{\lambda}, A) = \sum_{i=1}^{K} C_i \psi_i(\boldsymbol{\rho}, \boldsymbol{\lambda}, A^i), \quad \psi_i(\boldsymbol{\rho}, \boldsymbol{\lambda}, A^i)$$
$$= e^{-\frac{1}{2}(A_{11}^i \rho^2 + 2A_{12}^i \boldsymbol{\rho}\boldsymbol{\lambda} + A_{22}^i \lambda^2)}, \tag{2}$$

where C_i are linear variational parameters, A^i is the matrix of nonlinear variational parameters, and K is the basis size.

In the nonrelativistic approximation the Hamiltonian of a three-particle atom in Jacobi coordinates can be presented as

$$\hat{H}_0 = -\frac{1}{2\mu_1}\nabla_{\boldsymbol{\rho}}^2 - \frac{1}{2\mu_2}\nabla_{\boldsymbol{\lambda}}^2 + \frac{e_1 e_2}{|\boldsymbol{\rho}|} + \frac{e_1 e_3}{\left|\boldsymbol{\lambda} + \frac{m_2}{m_{12}}\boldsymbol{\rho}\right|}$$
$$+ \frac{e_2 e_3}{\left|\boldsymbol{\lambda} - \frac{m_1}{m_{12}}\boldsymbol{\rho}\right|}, \tag{3}$$

where $m_{12} = m_1 + m_2$, $\mu_1 = \frac{m_1 m_2}{m_1 + m_2}$, $\mu_2 = \frac{(m_1 + m_2)m_3}{m_1 + m_2 + m_3}$, and e_1, e_2, and e_3 are the particle charges.

For arbitrary states of the meson and electron with orbital angular momenta l_1 and l_2, a convenient basis for the expansion of functions depending on two directions are bipolar spherical harmonics [32]:

$$\left[Y_{l_1}(\theta_\rho, \phi_\rho) \otimes Y_{l_2}(\theta_\lambda, \phi_\lambda)\right]_{LM}$$
$$= \sum_{m_1, m_2} C_{l_1 m_1 l_2 m_2}^{LM} Y_{l_1 m_1}(\theta_\rho, \phi_\rho) Y_{l_2 m_2}(\theta_\lambda, \phi_\lambda), \tag{4}$$

where θ_ρ, ϕ_ρ and θ_λ, ϕ_λ are spherical angles that determine the direction of the vectors $\boldsymbol{\rho}$ and $\boldsymbol{\lambda}$, respectively. Since the π^- or K^- meson is in an orbital excited state l in pionic or kaonic helium and the electron is in the ground state, the variational wave function of the system is chosen for such states in the

form

$$\Psi_{lm}(\boldsymbol{\rho}, \boldsymbol{\lambda}, A) = \sum_{i=1}^{K} C_i Y_{lm}(\theta_\rho, \phi_\rho) \rho^l e^{-\frac{1}{2}(A_{11}^i \rho^2 + 2A_{12}^i \boldsymbol{\rho}\boldsymbol{\lambda} + A_{22}^i \lambda^2)}, \tag{5}$$

where the spherical function $Y_{lm}(\theta_\rho, \phi_\rho)$ describes the angular part of the orbital motion of a pion or kaon.

Within the framework of the variational approach, the solution of the Schrödinger equation is reduced to solving the following matrix problem for the coefficients C_i:

$$HC = EBC, \tag{6}$$

where the matrix elements of the Hamiltonian H_{ij} and normalizations B_{ij} can be calculated analytically in the basis of the Gaussian wave functions. Thus, the normalization of the wave function (5) is determined by the following expression:

$$\langle \Psi | \Psi \rangle = \sum_{i,j=1}^{K} C_i C_j 2^{l+2} \pi^{3/2} \Gamma\left(l + \frac{3}{2}\right) \frac{B_{22}^l}{(\det B)^{l+\frac{3}{2}}},$$
$$B_{kn} = A_{kn}^i + A_{kn}^j, \tag{7}$$

where $\Gamma(l + 3/2)$ is the Euler gamma function.

Consider further analytical results for the matrix elements of the Hamiltonian. The kinetic-energy operator contains two terms. The matrix element from the Laplace operator with respect to $\boldsymbol{\lambda}$ has the form

$$\langle \Psi | \nabla_{\boldsymbol{\lambda}}^2 | \Psi \rangle = \sum_{i,j=1}^{K} C_i C_j 2^{l+2} \pi^{\frac{3}{2}} \Gamma\left(l + \frac{3}{2}\right) \frac{B_{22}^{l-1}}{(\det B)^{l+\frac{5}{2}}}$$
$$\times \left[3A_{22}^i(A_{22}^i - B_{22})\det B + (2l+3)\right.$$
$$\left. \times (A_{22}^i B_{12} - A_{12}^i B_{22})^2\right]. \tag{8}$$

A similar matrix element with the Laplace operator in $\boldsymbol{\rho}$ is also expressed in terms of nonlinear variational parameters as follows:

$$\langle \Psi | \nabla_{\boldsymbol{\rho}}^2 | \Psi \rangle = \sum_{i,j=1}^{K} C_i C_j 2^{l+1} \pi^{\frac{3}{2}} \Gamma\left(l + \frac{1}{2}\right) \frac{B_{22}^{l-1}}{(\det B)^{l+\frac{5}{2}}}$$
$$\times \left\{(2l+1)\det B\left[-(2l+3)A_{11}^i B_{22} + 3(A_{12}^i)^2\right.\right.$$
$$\left. + 2lA_{12}^i B_{12}\right] + (2l+1)(2l+3)$$
$$\left. \times (A_{12}^i B_{12} - A_{11}^i B_{22})^2\right\}. \tag{9}$$

The potential-energy operator in the nonrelativistic Hamiltonian consists of pairwise Coulomb interactions U_{ij} ($i, j = 1, 2, 3$). The convenience of using the Gaussian basis in this case also lies in the possibility of an analytical representation of the matrix elements of the potential energy [in electron atomic units (e.a.u.)]:

$$\langle \Psi | U_{12} | \Psi \rangle = -Z \sum_{i,j=1}^{K} C_i C_j 2^{l+\frac{3}{2}} \pi^{\frac{3}{2}} \Gamma(l+1) \frac{B_{22}^{l-1}}{(\det B)^{l+1}}, \tag{10}$$

$$\langle \Psi | U_{13} | \Psi \rangle = -Z \sum_{i,j=1}^{K} C_i C_j 2^{l+\frac{5}{2}} \pi \Gamma\left(l + \frac{3}{2}\right) \frac{B_{22}^{l+\frac{1}{2}}}{(\det B)^{l+\frac{3}{2}}}$$
$$\times {}_2F_1\left(\frac{1}{2}, l + \frac{3}{2}, \frac{3}{2}, -\frac{(F_2^{23})^2}{\det B}\right), \tag{11}$$

TABLE I. Energy levels of the meson atom obtained in the nonrelativistic approximation with the Gaussian (G) and exponential (Exp) bases and values of the main corrections in the energy spectrum in electron atomic units.

State	E_{nr}(Exp)	E_{nr}(G)	$-\frac{\alpha^2}{8}\mathbf{p}_e^4$	ΔU_{vp}	ΔU_{cont}
		($^3_2$He -π^--e) atom			
(17, 16)	−2.64312261030188(2) [4]	−2.64238222	−0.00035742	−0.00000036	0.00000212
(17, 15)	−2.6709980910(1) [4]	−2.66982848	−0.00036341	−0.00000036	0.00000215
(18, 17)	−2.52088142679 [4]	−2.52053250	−0.00040763	−0.00000042	0.00000481
(18, 16)	−2.545645472099(1) [4]	−2.54506684	−0.00040557	−0.00000042	0.00000478
(19, 18)	−2.4329808449305 [4]	−2.43282621	−0.00045014	−0.00000045	0.00000529
(19, 17)	−2.4529359745011 [4]	−2.45265164	−0.00044052	−0.00000044	0.00000516
		($^4_2$He -π^--e) atom			
(17, 16)	−2.65751243850171 [4]	−2.65676897	−0.00035246	−0.00000035	0.00000209
(17, 15)	−2.68542722(2) [4]	−2.68424220	−0.00035923	−0.00000036	0.00000212
(18, 17)	−2.5319465695913 [4]	−2.53159626	−0.00040322	−0.00000041	0.00000475
(18, 16)	−2.556984919572(2) [4]	−2.55640530	−0.00040184	−0.00000041	0.00000473
(19, 18)	−2.4413857971745 [4]	−2.44123203	−0.00044557	−0.00000045	0.00000524
(19, 17)	−2.4618067856861 [4]	−2.46151679	−0.00043725	−0.00000044	0.00000514
		($^3_2$He -K^--e) atom			
(20, 19)	−4.70032469	−4.68062221	−0.00012207	−0.00000013	0.00000075
(20, 18)	−4.70435047	−4.69322183	−0.00011231	−0.00000012	0.00000068
(21, 20)	−4.31990309	−4.31336107	−0.00014995	−0.00000015	0.00000086
(21, 19)	−4.32856055	−4.32386298	−0.00014501	−0.00000015	0.00000088
(29, 28)	−2.74459354	−2.74407984	−0.00031887	−0.00000034	0.00000380
(29, 27)	−2.76135247	−2.76071139	−0.00032067	−0.00000034	0.00000380
(30, 29)	−2.65386695	−2.65349887	−0.00034777	−0.00000036	0.00000412
(30, 28)	−2.67027220	−2.66981800	−0.00035322	−0.00000037	0.00000418
		($^4_2$He -K^--e) atom			
(20, 19)	−4.83371129	−4.83289366	−0.00011988	−0.00000012	0.00000073
(20, 18)	−4.86241602	−4.85784789	−0.00010846	−0.00000012	0.00000066
(21, 20)	−4.45731745	−4.44998430	−0.00013049	−0.00000015	0.00000088
(21, 19)	−4.46536310	−4.46016857	−0.00013805	−0.00000014	0.00000083
(29, 28)	−2.80020575	−2.79967013	−0.00030251	−0.00000032	0.00000361
(29, 27)	−2.81647989	−2.81605377	−0.00031142	−0.00000034	0.00000370
(30, 29)	−2.70241808	−2.70204219	−0.00033248	−0.00000035	0.00000395
(30, 28)	−2.71878216	−2.71833449	−0.00033771	−0.00000036	0.00000400

$$\langle\Psi|U_{23}|\Psi\rangle = \sum_{i,j=1}^{K} C_i C_j 2^{l+\frac{5}{2}} \pi \Gamma\left(l+\frac{3}{2}\right) \frac{B_{22}^{l+\frac{1}{2}}}{(\det B)^{l+\frac{3}{2}}}$$

$$\times \, _2F_1\left(\frac{1}{2}, l+\frac{3}{2}, \frac{3}{2}, -\frac{\left(F_2^{13}\right)^2}{\det B}\right), \qquad (12)$$

$$F_2^{13} = B_{12} + \frac{m_1}{m_{12}} B_{22}, \quad F_2^{23} = B_{12} - \frac{m_2}{m_{12}} B_{22}, \qquad (13)$$

where $_2F_1(\alpha, \beta, x)$ is a hypergeometric function.

For $l = 1$ expressions (11)–(13) coincide with previously obtained results [33]. Using the matrix elements of the $\hat{H}_0$ Hamiltonian, some energy levels of the π^--meson and K^--meson atoms are calculated in the MATLAB system. The calculations are carried out using our program, which was previously used to calculate the energy levels of various muonic atoms in quantum electrodynamics. The calculation of the energy levels of the π^--meson atom is carried out in order

to test the operation of the program. The calculation results are shown in Table I.

To improve the accuracy of the calculation, we consider some important corrections to the Hamiltonian $\hat{H}_0$. The pair electromagnetic interaction between particles in quantum electrodynamics is determined by the Breit potential [34]. Among the various terms in this potential, let us single out those terms that have the greatest numerical value. They include relativistic corrections, contact interaction, and corrections for vacuum polarization.

The relativistic corrections are defined in the energy spectrum by the following terms in electron atomic units:

$$\Delta U_{rel} = -\frac{\alpha^2}{8}\left(\frac{\mathbf{p}_1^4}{m_1^3} + \frac{\mathbf{p}_2^4}{m_2^3} + \frac{\mathbf{p}_3^4}{m_3^3}\right). \qquad (14)$$

The term of leading order in (14) is related to the motion of the electron. The value of the matrix element from ΔU_{rel}^e can be obtained in exactly the same way as (8) in terms of
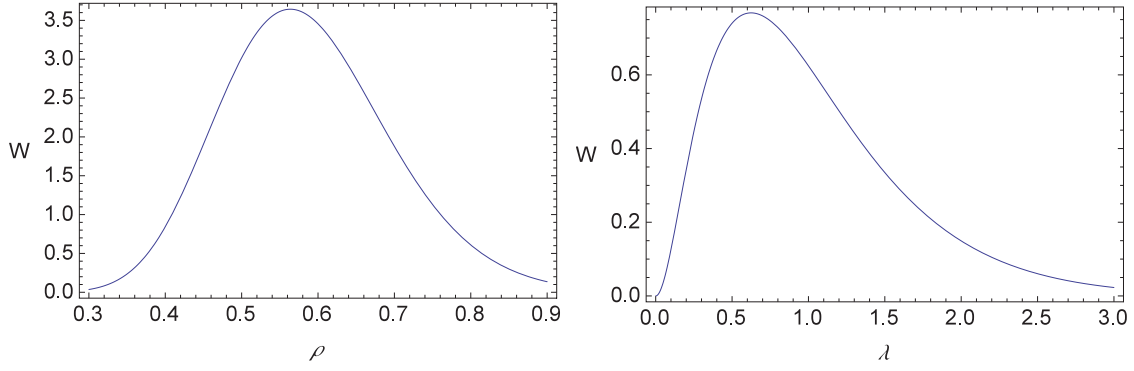
FIG. 1. The radial distribution densities $W(\rho)$ (left) and $W(\lambda)$ (right) for $(_2^3\text{He-}\pi^--e)$ for state (16,15). The values of variables ρ and λ are taken in electron atomic units.

variational parameters:

$$\langle\Psi|-\frac{\alpha^2}{8}\nabla_\lambda^4|\Psi\rangle = -\frac{\alpha^2}{8}\sum_{i,j=1}^{K}C_iC_j2^{l+2}\pi^{\frac{3}{2}}\Gamma\left(l+\frac{3}{2}\right)\frac{B_{22}^{l-2}}{(\det B)^{l+\frac{7}{2}}}\left[15\left(A_{22}^i\right)^2(\det B)^2\left(A_{22}^i-B_{22}\right)^2+10(2l+3)A_{22}^i\left(A_{22}^i-B_{22}\right)\right.$$

$$\left.\times\det B\left(A_{22}^iB_{12}-A_{12}^iB_{22}\right)^2+(2l+3)(2l+5)\left(A_{22}^iB_{12}-A_{12}^iB_{22}\right)^4\right]. \tag{15}$$

Let us also take into account the vacuum polarization effects in the energy spectrum. Since for both an electron and a meson in a highly excited state the Compton wavelength of an electron is much smaller than the radius of the Bohr orbit, we can use the following expression for the vacuum polarization potential in electron atomic units:

$$\Delta U_{\text{vp}} = \Delta U_{\text{vp}}(r_{13}) + \Delta U_{\text{vp}}(r_{23}) = -\frac{4}{15}\alpha^2(Z\alpha)\delta\left(\lambda+\frac{m_2}{m_{12}}\rho\right)+\frac{4}{15}\alpha^2(Z\alpha)\delta\left(\lambda-\frac{m_1}{m_{12}}\rho\right). \tag{16}$$

The matrix elements of such potentials are calculated analytically in a closed form:

$$\langle\Psi|\Delta U_{\text{vp}}(r_{13})|\Psi\rangle = -\frac{4}{15}\alpha^2(Z\alpha)\sum_{i,j=1}^{K}C_iC_j2^{l+\frac{1}{2}}\Gamma\left(l+\frac{3}{2}\right)$$

$$\times\frac{1}{\left(F_1^{13}\right)^{l+\frac{3}{2}}}, \tag{17}$$

$$\langle\Psi|\Delta U_{\text{vp}}(r_{23})|\Psi\rangle = -\frac{4}{15}\alpha^2(Z\alpha)\sum_{i,j=1}^{K}C_iC_j2^{l+\frac{1}{2}}\Gamma\left(l+\frac{3}{2}\right)$$

$$\times\frac{1}{\left(F_1^{23}\right)^{l+\frac{3}{2}}}, \tag{18}$$

$$F_1^{13} = B_{11}+\frac{m_2^2}{m_{12}^2}B_{22}-2\frac{m_2}{m_{12}}B_{12},$$

$$F_1^{23} = B_{11}+\frac{m_1^2}{m_{12}^2}B_{22}+2\frac{m_1}{m_{12}}B_{12}. \tag{19}$$

The contact interaction potential, as well as (16), is expressed through the δ functions in the form (in electron atomic units)

$$\Delta U_{\text{cont}} = \frac{\pi Z\alpha^2}{2}\delta\left(\lambda+\frac{m_2}{m_{12}}\rho\right)-\frac{\pi\alpha^2}{2}\delta\left(\lambda-\frac{m_1}{m_{12}}\rho\right). \tag{20}$$

In Table I we present the results from calculating the energy values with the Hamiltonian $\hat{H}_0$ and the values of the matrix elements (15), (17), (18), and (20).

The obtained wave functions (5) make it possible to calculate the radial distribution densities in ρ and λ and root-mean-square values $\sqrt{\langle\rho^2\rangle}$ and $\sqrt{\langle\lambda^2\rangle}$, which are determined by the expressions

$$W(\rho) = \frac{(2\pi)^{3/2}}{\langle\Psi|\Psi\rangle}\sum_{i,j=1}^{K}\frac{C_iC_j}{B_{22}^{3/2}}\rho^{(2l+2)}e^{-\frac{1}{2}\frac{\det B}{B_{22}}\rho^2}, \tag{21}$$

$$W(\lambda) = \frac{2^{l+\frac{5}{3}}\pi}{\langle\Psi|\Psi\rangle}\sum_{i,j=1}^{K}\frac{C_iC_j\Gamma\left(l+\frac{3}{2}\right)}{B_{11}^{l+\frac{3}{2}}}\lambda^2e^{-\frac{1}{2}B_{22}\lambda^2}$$

$$\times {}_1F_1\left(l+\frac{3}{2},\frac{3}{2},\frac{B_{12}^2\lambda^2}{2B_{11}}\right), \tag{22}$$

$$W(\rho,\lambda) = \frac{4\pi}{\langle\Psi|\Psi\rangle}\sum_{i,j=1}^{K}\frac{C_iC_j}{B_{12}}\rho^{2l+1}\lambda e^{-\frac{1}{2}[B_{11}\rho^2+B_{22}\lambda^2]}sh(B_{12}\rho\lambda),$$

$$B_{lk} = A_{lk}^i+A_{lk}^j, \tag{23}$$

$$\langle\rho^2\rangle = \frac{\pi^{\frac{3}{2}}2^{l+3}\Gamma\left(l+\frac{5}{2}\right)}{\langle\Psi|\Psi\rangle}\sum_{i,j=1}^{K}C_iC_j\frac{B_{22}^{l+1}}{(\det B)^{l+5/2}}, \tag{24}$$

$$\langle\lambda^2\rangle = \frac{\pi^{\frac{3}{2}}2^{l+2}\Gamma\left(l+\frac{3}{2}\right)}{\langle\Psi|\Psi\rangle}\sum_{i,j=1}^{K}C_iC_j\frac{B_{22}^{l-1}}{(\det B)^{l+\frac{5}{2}}}$$
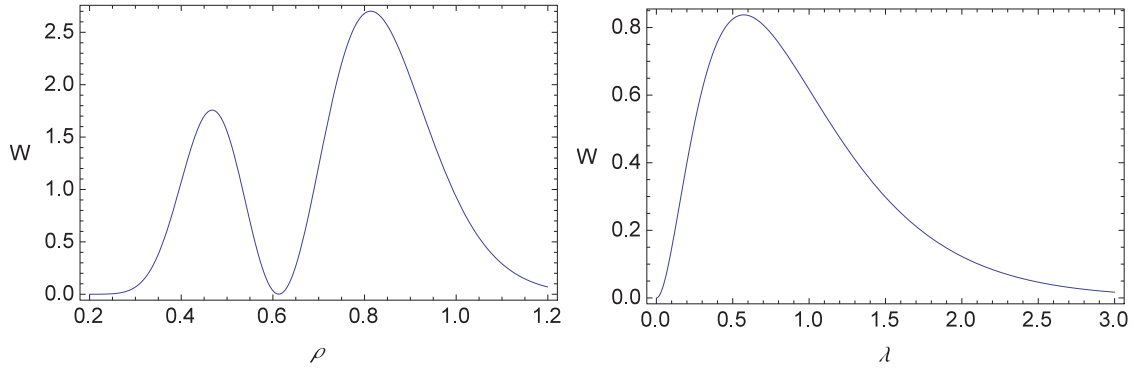
$$\times\left(3B_{11}B_{22}+2B_{12}^2l\right). \tag{25}$$

FIG. 2. The radial distribution densities $W(\rho)$ (left) and $W(\lambda)$ (right) for $(_2^3\text{He-}\pi^--e)$ for state (17,15). The values of variables ρ and λ are taken in electron atomic units.

The radial distribution densities are presented in Figs. 1–4 in the cases of pionic helium and kaonic helium. These plots show the presence of characteristic distances in the particle systems (He-π^--e) and (He-K^--e). It also follows from these graphs that for the considered states, the meson turns out to be located the same distance from the nucleus or slightly closer to the nucleus than the electron. The distribution densities for the two radial variables ρ and λ provide a more complete picture of the characteristic distances in a given system of three particles. They are shown in two graphs in Figs. 5 and 6.

Fine splitting in a three-particle atom which is determined by the interaction of the electron spin and the large orbital angular momentum of the meson is not considered here.

III. DISCUSSION OF THE RESULTS

To calculate the energy of a specific state, we run the program 10 different times with a minimum basis of 200 functions, varying the boundaries to generate nonlinear variational parameters. Having selected the boundaries where the minimum energy is obtained at this stage, we launch several programs with the same parameters, increasing the basis to approximately 800 functions. At each step of the program, the basis is increased by one, and refinement cycles are performed. The number of such cycles (usually, this value is 1000) is specified in the input file at the beginning of the pro-

gram. The final size of the basis is not limited, but the program ends when it cannot refine the minimum energy obtained in the previous step. By making several such calculations, we determine by what amount the results change. We take the number of matching digits as the accuracy of our calculations. We present the calculation results by writing the energy to eight decimal places, which determines the accuracy of the calculation in our approach. Of course, there are a number of other corrections in the three-particle interaction potential that are not accounted for, but they are suppressed by the additional degree of the fine-structure constant α. Thus, it is possible to determine the accuracy of the calculation by taking into account uncalculated corrections of 10^{-7} e.a.u.

This paper examines the energy levels of pionic and kaonic helium for states in which the meson has such a large orbital momentum that it is located approximately the same distance from the nucleus as the electron. The calculations are performed in leading order within the framework of the variational method with the Gaussian basis, and a number of basic corrections determined by the Breit Hamiltonian (for relativism, vacuum polarization, and contact interaction) are calculated in the first order of perturbation theory. Since an electron is in the $1S$ state, the notation (n, l) is used for a state with three particles in Table I, where l is the orbital momentum of the meson and n is the principal quantum number of subsystem (π^-He^{2+}) or (K^-He^{2+}). In our case the variational trial function is restricted to the subspace of
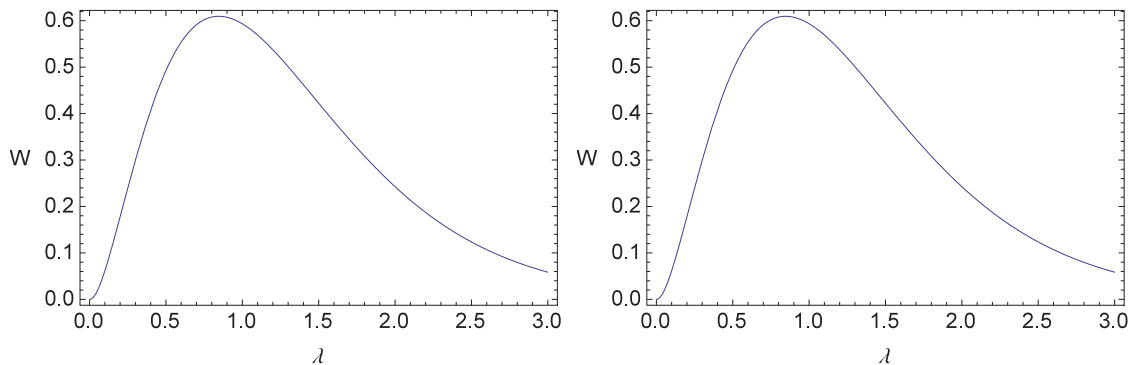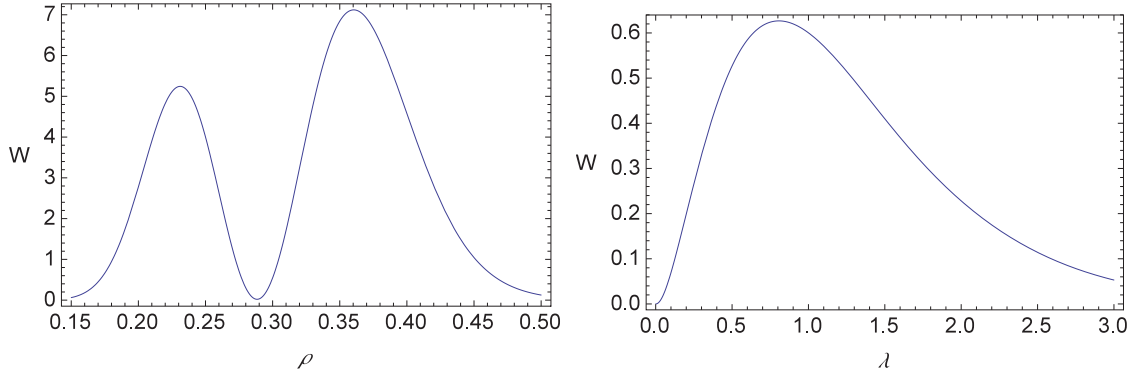

FIG. 3. The radial distribution densities $W(\rho)$ (left) and $W(\lambda)$ (right) for $(_2^3\text{He-}K^--e)$ for state (21,20). The values of variables ρ and λ are taken in electron atomic units.

FIG. 4. The radial distribution densities $W(\rho)$ (left) and $W(\lambda)$ (right) for $(^3_2\text{He-}K^- \text{-} e)$ for state (22,20). The values of variables ρ and λ are taken in electron atomic units.

σ states [for states with an azimuthal quantum number of an electron in the moving frame equal to zero, see Eq. (5)]. In this case the states of interest become bound, and the standard variational procedure is valid. These issues were discussed in our previous works [35,36], which showed that the problem is reduced (projected) to Feshbach-type closed-channel equations.

The Rydberg states in atoms play an important role in refining the values of fundamental constants. Thus, based on the spectroscopy of the Rydberg states in a hydrogen atom, the measurement of the Rydberg constant has been improved [37,38]. In this problem, by working with the Rydberg states, it is possible to eliminate contributions to the structure of a
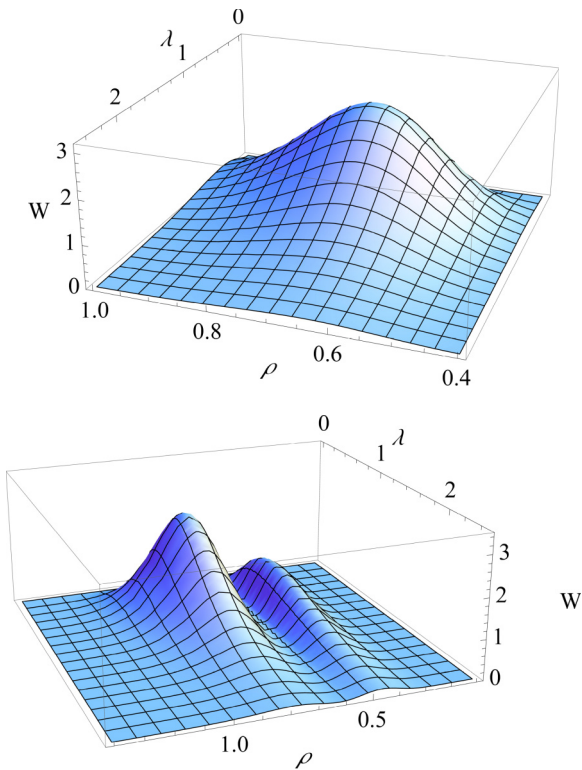

FIG. 5. The radial distribution density $W(\rho, \lambda)$ for $(\pi e\, ^4\text{He})$ in states (17,16) (top) and (17,15) (bottom). The values of variables ρ and λ are taken in electron atomic units.

nucleus. In the case of mesonic atoms, the use of Rydberg states makes it possible to reduce the influence of strong interaction on the energy spectrum.

Spectroscopy of various exotic molecules can provide new information about the nature of fundamental interactions and the values of fundamental parameters of the standard model. Several years ago, the PiHe collaboration at the Paul Scherrer Institute performed laser spectroscopy of the infrared transition in three-body pion helium atoms [4,5]. The atoms were created in a superfluid (He II) helium target. Similar measurements in antiproton helium atoms embedded in liquid helium were carried out by the CERN Atomic Spectroscopy And Collisions Using Slow Antiprotons collaboration [39]. The antiproton-to-electron mass ratio was determined as $m_p/m_e = 1836.1526734(15)$ [39]. The mass of π mesons can be determined by comparing the experimental transition frequencies in pionic helium with the results of the QED calculation [4]. Although the transition frequency $(17, 16) \rightarrow (17, 15)$ has already been measured for pionic helium [5], the analysis of experimental data to extract the pion mass is still ongoing.

Our study of the energy levels of both pionic and kaonic helium is carried out on the basis of the variational approach, which was developed in Ref. [28]. In contrast to Ref. [4], to describe a three-particle system, the Jacobi coordinates $\boldsymbol{\rho}$ and $\boldsymbol{\lambda}$ are used, in which the original Hamiltonian has the form (3). The second difference between our calculation and [4] is the use of a Gaussian basis rather than an exponential basis within the variational method. In such a basis, all matrix elements of the Hamiltonian are obtained in a closed analytical form. In the case of an exponential basis, the calculation of matrix elements can also be performed analytically, but very often, when a calculation program is written, the calculation of such matrix elements is performed numerically. Finally, the third difference between our calculations and [4] is that in [4], within the framework of the variational approach, the method of complex coordinate rotation is used, and we work with a real Hamiltonian and solve the eigenvalue problem (6). The obtained numerical results for the leading-order contribution to the energy of the system and corrections to it are presented in Table I. Comparing these results with calculation in [4], it is necessary to note a slight difference in the results which appears in the third digit after the decimal point (second column in Table I). For the $(17.16) \rightarrow (17.15)$ transition frequency for pionic ^{4}He that was measured, our result
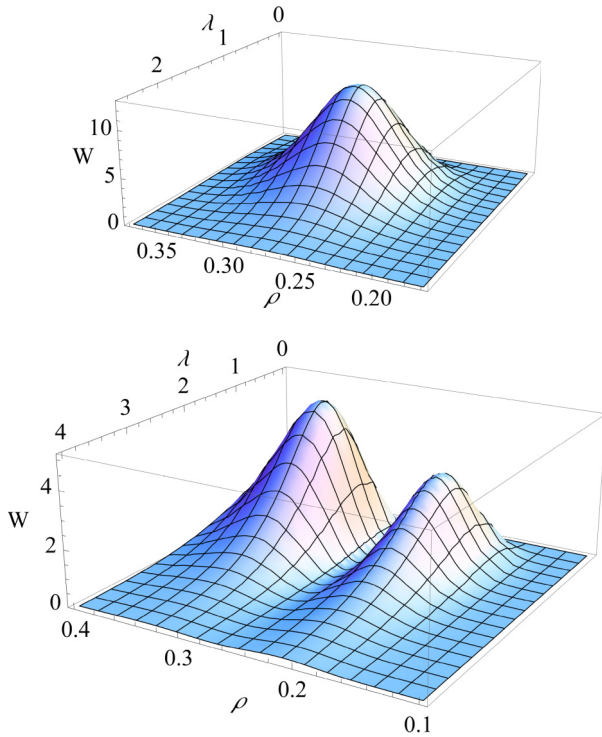
FIG. 6. The radial distribution density $W(\rho, \lambda)$ for $(Ke\,^3\mathrm{He})$ in states (21,20) (top) and (21,19) (bottom). The values of variables ρ and λ are taken in electron atomic units.

180 772 GHz is slightly different (close to 1%) from the result $183\,681.5 \pm 0.5$ GHz obtained in [4] and from the experimental value, which is 183 760(6) (6) GHz. Our result for a similar transition frequency in pionic $^3\mathrm{He}$ is 180 594 GHz. We also present here the results for the $(21, 20) \rightarrow (21, 19)$ transition frequencies in the case of kaonic helium. They are 69 094 GHz $(K\text{-}e\text{-}\frac{3}{2}\mathrm{He})$ and 67 017 GHz $(K\text{-}e\text{-}\frac{4}{2}\mathrm{He})$. In general, our results using the Gaussian trial functions (third column of Table I) are consistent with calculations with an exponential basis in [4] (second column of Table I) in the case of pionic helium. In the case of kaonic helium, we obtained results using an exponential and Gaussian basis. The difference in results is due, in our opinion, to differences in the variational approaches used in this work and in [4] and the bases for variational wave functions.

A study of the characteristic distances at which the nucleus, meson, and electron are located relative to each other is shown in Figs. 1–6 for some states for which the binding energies are calculated. The meson is in an excited state with a large orbital momentum l. The key parameter with which one can estimate its distance to the nucleus is determined by the expression $\sqrt{\mu_1/m_3}$, where μ_1 is the reduced mass of the meson-nucleus system and m_3 is the electron mass. When the principal quantum number $n = \sqrt{\mu_1/m_3} \approx 16$ for the $(\pi^- \,\frac{4}{2}\mathrm{He})$ or $(\pi^- \,\frac{3}{2}\mathrm{He})$ subsystem, the movement of the π^- meson occurs at approximately the same distance from the nucleus and has the same binding energy as the electron. In the case of kaonic helium, the value of the principal quantum number increases due to an increase in the meson mass and reaches the value $n \approx 29$. This parameter determines the order of the principal quantum number n at which the meson and electron have close orbits. But in this work we have so far considered slightly smaller values, $n \approx 20$, so that the K^- meson is located a little closer to the nucleus. It follows from Figs. 1–6 that in the case of the considered Rydberg states of the π^- or K^- meson, characteristic distances along ρ and λ have close values. So, for example, the root-mean-square value of $\sqrt{\lambda^2}$ for state (17,16) in $(\pi\text{-}e\text{-}\frac{4}{2}\mathrm{He})$ is 60 050 fm, and the root-mean-square value of $\sqrt{\rho^2}$ for the same state is 37 210 fm. This means that the use of an analytical method to calculate energy levels as in [13,21] is difficult since the characteristic series for the parameter M_e/M_μ from [13,21] does not rapidly converge.

When calculating relativistic effects, we take into account only the corresponding correction for the electron, meaning that the electron is the lightest particle in this system, and with an increase in the principal quantum number n, the orbital speed is determined by the formula $v = Z\alpha/n$. Therefore, for a meson in circular Rydberg states it is suppressed by the factor n.

In Table I we limited ourselves to presenting numerical results from calculating the energies of bound states of three particles for only a certain number of states with (n, l). But the obtained general analytical formulas for the matrix elements of the Hamiltonian of the system make it possible to carry out corresponding numerical calculations for other states (n, l) which may be more important for the experiment. For the principal quantum number $n = 29$, the binding energy of kaonic helium in state $(n, l) = (29, 28)$ is equal to $-2.798\,355\,417\,6$ e.a.u., and in state $(n, l) = (29, 27)$ it has the value $-2.814\,521\,016\,7$ e.a.u., which ultimately gives the transition frequency between these levels, $\nu = 106\,364$ GHz.

[1] M. I. Eides, H. Grotch, and V. A. Shelyuto, Theory of light hydrogenlike atoms, Phys. Rep. **342**, 63 (2001).

[2] A. Antognini, F. Hagelstein, and V. Pascalutsa, The proton structure in and out of muonic hydrogen, Annu. Rev. Nucl. Part. Sci. **72**, 389 (2022).

[3] C. Pizzolotto, A. Adamczak, D. Bakalov, G. Baldazzi, and M. Baruzzo, The FAMU experiment: Muonic hydrogen high precision spectroscopy studies, Eur. Phys. J. A **56**, 185 (2020).

[4] M. Hori, A. Soter, and V. I. Korobov, Proposed method for laser spectroscopy of pionic helium atoms to determine the charged-pion mass, Phys. Rev. A **89**, 042515 (2014).

[5] M. Hori, A. Sótér, H. Aghai-Khozani, D. Barna, A. Dax, R. S. Hayano, Y. Murakami, and H. Yamada, Method for laser spectroscopy of metastable pionic helium atoms, Hyperfine Interact. **233**, 83 (2015).

[6] M. Hori, H. Aghai-Khozani, A. Soter, A. Dax, and D. Barna, Laser spectroscopy of pionic helium atoms, Nature (London) **581**, 37 (2020).

[7] M. Hori, H. Aghai-Khozani, A. Sótér, A. Dax, D. Barna, and L. Venturelli, Laser spectroscopy of long-lived pionic and antiprotonic helium in superfluid helium, PoS **ICHEP2022**, 141 (2022).

[8] D. Bakalov, Calculation of the density shift and broadening of the transition lines in pionic helium: Computational problems, Hyperfine Interact. **233**, 127 (2015).

[9] B. Obreshkov, *Systematic Effects in the Measurement of the Negatively Charged Pion Mass Using Laser Spectroscopy of Pionic Helium Atoms*, edited by M. Gaidarov and N. Minkov, Nuclear Theory Vol. 35 (Heron, Sofia, 2016).

[10] B. Obreshkov and D. Bakalov, Collisional shift and broadening of the transition lines in pionic helium, Phys. Rev. A **93**, 062505 (2016).

[11] M. Trassinelli, D. F. Anagnostopoulos, G. Borchert, A. Dax, J.-P. Eggerr, D. Gotta, M. Hennebach, P. Indelicato, Y.-W. Liu, B. Manil, N. Nelms, L.M. Simons, and A. Wells, Measurement of the charged pion mass using x-ray spectroscopy of exotic atoms, Phys. Lett. B **759**, 583 (2016).

[12] R. L. Workman *et al.* (Particle Data Group), Review of particle physics, Prog. Theor. Exp. Phys. **2022**, 083C01 (2022).

[13] A. V. Eskin, V. I. Korobov, A. P. Martynenko, and F. A. Martynenko, Energy levels of three-particle muon electron helium in variational approach, Phys. At. Nucl. **86**, 583 (2023).

[14] V. I. Korobov, A. P. Martynenko, F. A. Martynenko, and A. V. Eskin, Muon Lamb shift in three-particle muon electron systems in quantum electrodynamics, Bull. Lebedev Phys. Inst. **50**, 229 (2023).

[15] A. V. Eskin, V. I. Korobov, A. P. Martynenko, and F. A. Martynenko, Three particle muon electron bound systems in quantum electrodynamics, Atoms **11**, 25 (2023).

[16] S. D. Lakdawala and P. Mohr, Hyperfine structure in muonic helium, Phys. Rev. A **22**, 1572 (1980).

[17] K. N. Huang and V. W. Hughes, Theoretical hyperfine structure of the muonic ^{3}He and ^{4}He atoms, Phys. Rev. A **26**, 2330 (1982).

[18] M. Y. Amusia, M. J. Kuchiev, and V. L. Yakhontov, Computation of the hyperfine structure in the $(\alpha - \mu^- e^-)^0$ atom, J. Phys. B **16**, L71 (1983).

[19] S. G. Karshenboim, V. G. Ivanov, and M. Y. Amusia, Lamb shift of electronic states in neutral muonic helium, an electron-muon-nucleus system, Phys. Rev. A **91**, 032510 (2015).

[20] A. A. Krutov and A. P. Martynenko, Ground-state hyperfine structure of the muonic helium atom, Phys. Rev. A **78**, 032513 (2008).

[21] R. N. Faustov, V. I. Korobov, A. P. Martynenko, and F. A. Martynenko, Ground-state hyperfine structure of light muon-electron ions, Phys. Rev. A **105**, 042816 (2022).

[22] R. J. Drachman, Nobrelativistic hyperfine splitting in muonic helium by adiabatic perturbation theory, Phys. Rev. A **22**, 1755 (1980).

[23] S. I. Vinitsky, V. S. Melezhik, L. I. Ponomarev *et al.*, Calculation of energy levels of hydrogen isotope μ mesic molecules in the adiabatic representation of three-body problem, Sov. Phys. JETP **52**, 353 (1980).

[24] A. M. Frolov, Properties and hyperfine structure of helium-muonic atoms, Phys. Rev. A **61**, 022509 (2000).

[25] A. M. Frolov, The hyperfine structure of the ground states in the helium-muonic atoms, Phys. Lett. A **376**, 2548 (2012).

[26] M.-K. Chen, Correlated wave functions and hyperfine splitting of the 2s state of muonic ^{3,4}He atoms, Phys. Rev. A **45**, 1479 (1992).

[27] H. Fatehizadeh, R. Gheisari, and H. Falinejad, Full calculation of $\mu p d$ and $\mu d t$ muonic bound levels: Combination of Nikiforov-Uvarov method and variational approach, Ann. Phys. (NY) **385**, 512 (2017)

[28] K. Varga and Y. Suzuki, Solution of few-body problems with the stochastic variational method I. Central forces with zero orbital momentum, Comput. Phys. Commun. **106**, 157 (1997).

[29] J. Mitroy, S. Bubin, W. Horiuchi, Y. Suzuki, L. Adamowicz, W. Cencek, K. Szalewicz, J. Komasa, D. Blume, and K. Varg, Theory and application of explicitly correlated Gaussians, Rev. Mod. Phys. **85**, 693 (2013).

[30] V. I. Korobov, Variational methods in the quantum three-body problem with Coulomb interaction, Phys. Part. Nuclei **53**, 1 (2022).

[31] M. A. Khan, Hyperspherical three-body calculation for exotic atoms, Few-Body Syst. **52**, 53 (2012).

[32] D. A. Varshalovich, A. N. Moskalev, and V. K. Khersonsky, *Quantum Theory of Angular Momentum* (World Scientific, Singapore, 1988).

[33] A. P. Martynenko, F. A. Martynenko, V. V. Sorokin, O. S. Sukhorukova, and A. V. Eskin, Energy levels of mesomolecular ions of hydrogen in variational approach, Bull. Lebedev Phys. Inst. **46**, 143 (2019).

[34] L. D. Landau and E. M. Lifshitz, *Quantum Electrodynamics*, 3rd ed, Course of Theoretical Physics Vol. 4, Moscow. Publishing house Fizmatlit, 2008 (Pergamon, New York, 1977).

[35] V. I. Korobov, Metastable states in the antiprotonic helium atom decaying via Auger transitions, Phys. Rev. A **67**, 062501 (2003).

[36] V. I. Korobov, Variational calculation of energy levels in $\bar{p}He^+$ molecular systems, Phys. Rev. A **54**, R1749 (1996).

[37] B. de Beauvoir, F. Nez, L. Julien, B. Cagnac, F. Biraben, D. Touahri, L. Hilico, O. Acef, A. Clairon, and J. J. Zondy, Absolute frequency measurement of the 2*S*-8*S/D* transitions in hydrogen and deuterium: New determination of the Rydberg constant, Phys. Rev. Lett. **78**, 440 (1997).

[38] C. Schwob, L. Jozefowski, B. de Beauvoir, L. Hilico, F. Nez, L. Julien, F. Biraben, O. Acef, J.-J. Zondy, and A. Clairon, Optical frequency measurement of the 2*S*-12*D* transitions in hydrogen and deuterium: Rydberg constant and Lamb shift determinations, Phys. Rev. Lett. **82**, 4960 (1999).

[39] A. Sóter, H. Aghai-Khozani, D. Barna, A. Dax, L. Venturelli, and M. Hori, High-resolution laser resonances of antiprotonic helium in superfluid ^{4}He, Nature (London) **603**, 411 (2022).